Scientific Research Publishing

Open Journal of Geology, 2026, 16(2), 73-84
https://www.scirp.org/journal/ojg
ISSN Online: 2161-7589
ISSN Print: 2161-7570

Geological Characterization of Fractures in the Structural and Tectonic Units of the Atacora Range in North-Western Benin

Ringo Fernand Avahounlin[1,2*], Jean-Eudes Okoundé[1], Lucie Koudérin[1], Renaud Mitchozounou[1], Luc Glodji Adissin[3], Kélomé Nelly[3]

[1]UNESCO International Chair of Physical Mathematics and Applications, Calavi, Benin
[2]Laboratory of Natural Sciences and Applications, Natitingou, Benin
[3]Department of Earth Sciences, Abomey-Calavi University, Calavi, Benin
Email: *d2ringofernand@gmail.com

How to cite this paper: Avahounlin, R.F., Okoundé, J.-E., Koudérin, L., Mitchozounou, R., Adissin, L.G. and Nelly, K. (2026) Geological Characterization of Fractures in the Structural and Tectonic Units of the Atacora Range in North-Western Benin. *Open Journal of Geology*, **16**, 73-84.
https://doi.org/10.4236/ojg.2026.162005

Received: August 22, 2025
Accepted: January 31, 2026
Published: February 3, 2026

Abstract

Access to groundwater, particularly in the base zone, is a real problem. Located in the northwest of Benin, the structural and tectonic units of the Atacora chain are composed of fractured sedimentary and crystalline formations. The objective of this study is to dimension fractures on the scale of the Atacora Tectonic Unit and its foreland. The Landsat OLI 09 TIRS images have been processed in order to enhance the linear elements considered as lineaments. The lineaments obtained were compared with high-flow drilling data in order to identify fractures in the lineament network. In total, 417 fractures of various sizes (0.33 - 34.10 km) and orientations (NNE-SSW, NE-SW, ENE-OSO, ESE-ONO, SE-NO, and SSE-NNO) were identified. The distribution of fracture orientations shows a certain heterogeneity of fracturing in the study area. The statistical analysis shows that the fractures are numbered in the ESE-WNW directions: 146 fractures of length between 0.5 - 34.10 km and density between 7.87×10^{-5} - 2.50×10^{-3} km/km^2; NE-SW, a total of 121 fractures with a length between 0.335 - 14.41 km and a density between 2.49×10^{-5} - 1.07×10^{-3} km/km^2; ENE-OSO, 91 fractures with a length between 0.5 - 14.10 km and density between 3.78×10^{-5} - 1.04×10^{-3} km/km^2; and for NNE-SSW, there are 39 fractures with a length between 0.33 - 6.74 km and a density between 2.88×10^{-5} - 5.01×10^{-3} km/km^2. All the results contribute to a better understanding of fracture networks and the functioning of groundwater in the structural and tectonic units of the Atacora chain.

Keywords

Characterization, Fracture, Structural Units, Atacora Range, North-West Benin

1. Introduction

The climatic conditions of the Atacora department (Sudanian type climate) provide rainfall amounts of around 1199 mm per year. These rains, in turn, generate infiltration of around 150 million m^3/year [1]. Although the Atacora department is blessed with relative wealth in water resources, it faces challenges in mobilizing them. Groundwater is the main source of drinking water supply; its occurrence and availability are governed by the existing relationship between factors intrinsic to the environment (hydrogeology, drainage network, fracturing, slope) [2] [3].

However, the exploitation of groundwater poses a problem in crystalline basement areas. Indeed, the hydrogeology of crystalline basement zones is very complex [4]. Groundwater capture has long focused on identifying geological structures for water production. In the basement areas, the hydrogeological characteristics of the crystalline rocks determine the recharge of the water tables and therefore the sustainability of the drilling carried out. A study carried out on nearly 5300 drillings showed that the success rate of drilling is 70% to 90% in the sedimentary zone, compared to around 60% in the basement [5]. The rocks of the crystalline and crystallophyllian zones are intrinsically very poorly permeable; it is the fractures that account for almost all of their permeability properties (depending on their density, size, and aperture) [6] [7]. The fracture network, both ancient and recent, constitutes one of the main parameters for characterizing hydrogeological systems in the basement environment. Their characteristics are likely to explain the hydraulic functioning of fractured environments [8] [9].

To our knowledge, there has been no work on the characterization of the fracture network in the study area. However, several works have been carried out on the characterization of fractures in the Beninese crystalline basement [10] [11] and in the Ivorian Paleozoic basement [12]-[14].

The structural and tectonic units of the Atacora range are located between longitudes 0˚45' and 2˚03' East and latitudes 9˚30' and 11˚30' North (**Figure 1(a)**). **Figure 1(b)** presents the altitudes, which reflect the terrain relief of the study area. In the area, altitudes decrease from East to West. This situation divides the study area into three sectors: eastern, middle, and western. In the eastern sector, altitudes vary between 302 m and 675 m and correspond to the domain of the Atacora mountain range, which belongs to the Pan-African Dahomeyid orogen. In the center, we approach a plain of piedmont and hills (206 - 301 m); this sector is characterized by medium altitudes and geologically corresponds to the Buem unit of the Dahomeyids chain. To the west, the altitudes are lower (128 - 205 m) with relatively gentle slopes; this sector corresponds morphologically to the Pendjari plain and geologically to the Volta basin.

Geologically, the structural and tectonic units of the Atacora range belong to the tectonic unit of Atacora and its foreland. It is subdivided into several areas, which are the Atacora Structural Unit, the Bueme, the Tiélé Structural Unit, and

the Volta Basin and its foreland (Figure 1(d)), which are from East to West. They outcrop sedimentary formations (sand, argillite, ancient and recent alluvium) and crystalline formations (sandstone, silistone, schist, jasper) (Figure 1(c)) [15]. The reconstruction of the genesis of the study area is broken down into three stages: the construction of a passive margin on the western edge of a Pan-African ocean; the collision of this passive margin with the Benino-Nigerian plate, giving rise to the Dahomeyid chain. These events contributed to the formation of a molassic basin at the foot of the Dahomeyid chain [16].

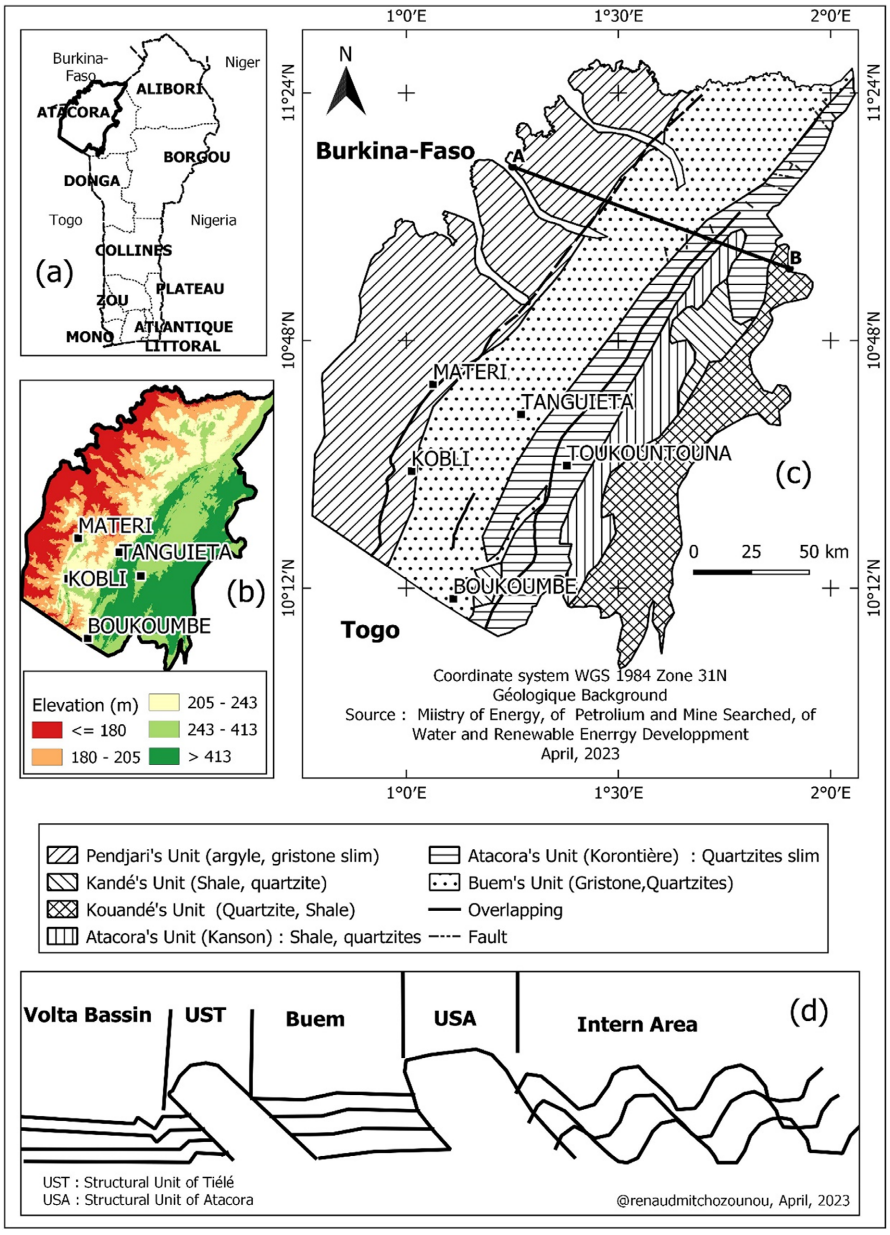

Figure 1. Presentation of the Atacora Structural Unit and its foreland: (a) Geographical location of Benin in West Africa; (b) Altitudes of the study area; (c) Geological map of the study area; (d) Geological profile of the units composing the structural and tectonic units of the Atacora chain and its foreland.

2. Data and Analysis Methods

Planimetric data consisting of satellite images (Landsat 09 type Oli Shots of scenes 193-52; 192-52; 193-53 and 192-53) and geological sheets (E: 1/200,000) of Natitingou, Porga, and Sansanne-Mango, associated with a series of drilling flow rates in the study area, were used to extract the lineaments. The different strips and scenes of the images were stacked, mosaicked, and then cleared. The clearance was carried out using statistics based on Principal Component Analysis (PCA) of the different image bands in order to eliminate redundant information [17] (**Figure 2**). Sobel filters of type 7 × 7 were applied to enhance and extract the lineaments obtained (**Figure 3**). These filters accentuate the lithological and structural discontinuities of the land surface along the N-S; E-O; NE-SW; and NW-SE directions, which enhances the perpendicular directional lineaments [14] [18] [19]. The abrupt discontinuities in tone observed on enhanced images are represented by straight segments [13]. A total of 775 lineaments were identified, including 10% in the WNW-ESE direction, 7% following the NNE-SSW direction, 7% following the NE-SW direction, and 5% following the NW-SE direction (**Figure 4(a)**).

To identify the fracture networks in the extracted lineaments, the major directions of the lineaments and those of the fractures revealed on the geological sheets were determined using the directional rosette and then compared with each other (**Figure 4**). The extracted lineaments whose major directions coincide with those of the revealed fractures would contain within them a network of fractures, which were then separated from the predefined lineaments. Fractures validated [14] [20] are those which follow the distribution of drilling (**Figure 5**) at medium or high flow rates. A total of 417 fractures were identified across the study area (**Figure 6**).

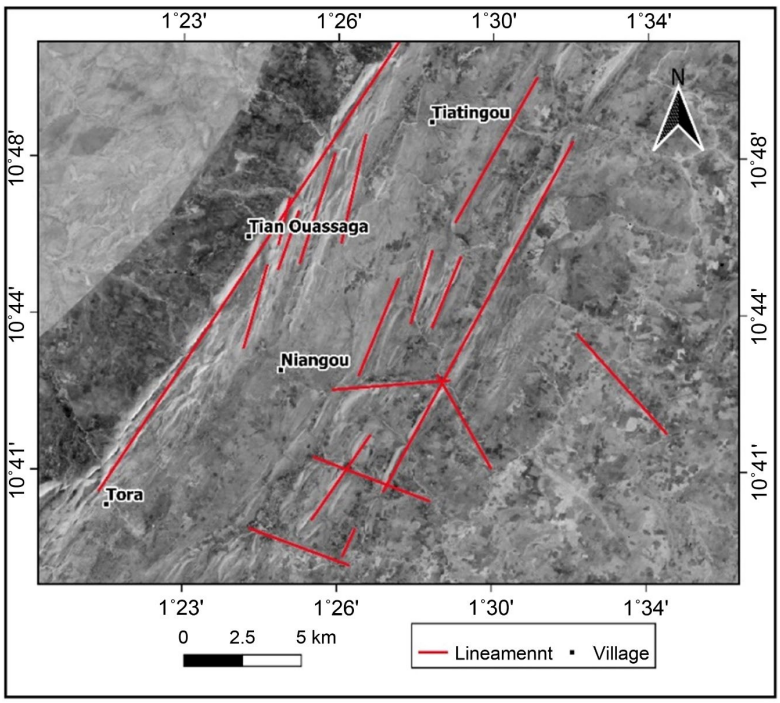

Figure 2. Lineaments visible on PCA.

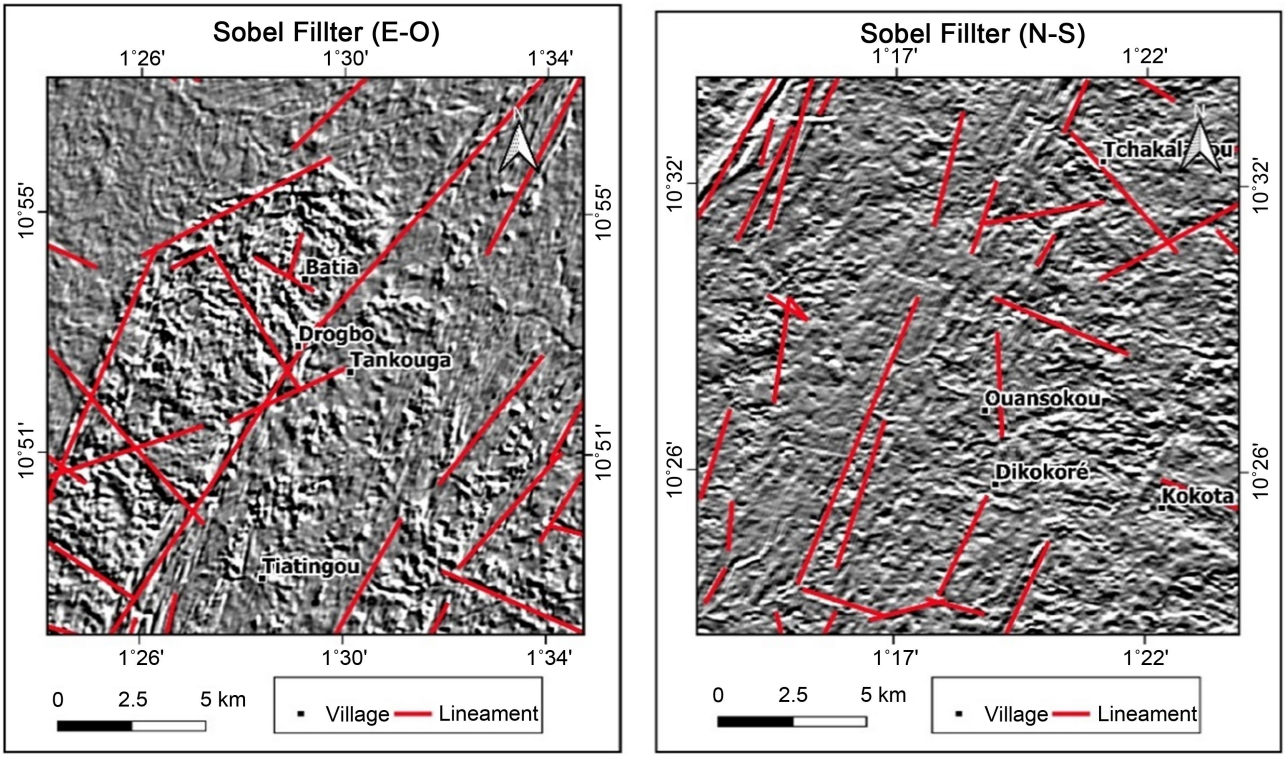

Figure 3. Sobel filters applied to images.

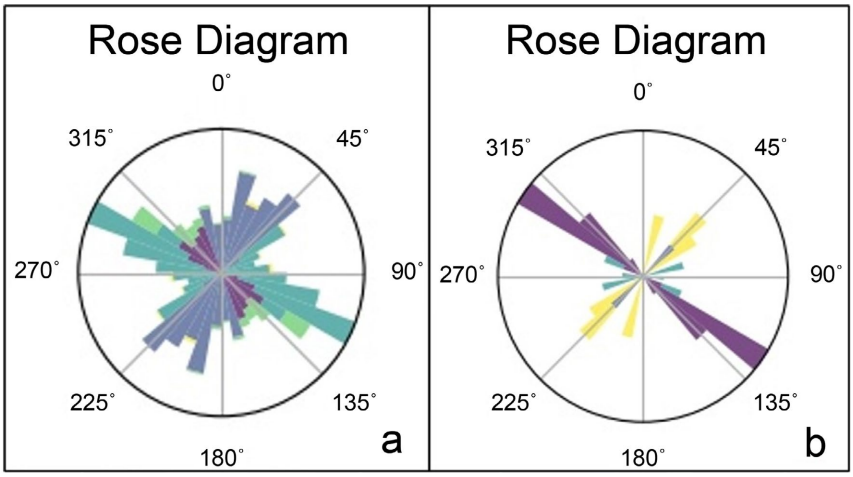

Figure 4. Directional rosette: (a) lineaments identified; (b) fractures revealed.

The orientation, density, and length of identified fractures were determined. The orientation of the fractures is indicated by the directional rosette. The lengths of the fractures are determined using the function of the Qgis 3.16 interface. The density of fractures is determined according to the expression [4] [19]:

$$Df = \frac{\sum_{i=1}^{n} L_i}{A} \quad (1)$$

with *Df*: density of fractures [km/km^2], L_i: total length of fractures in km, and *A*: surface area occupied by fractures in km^2.

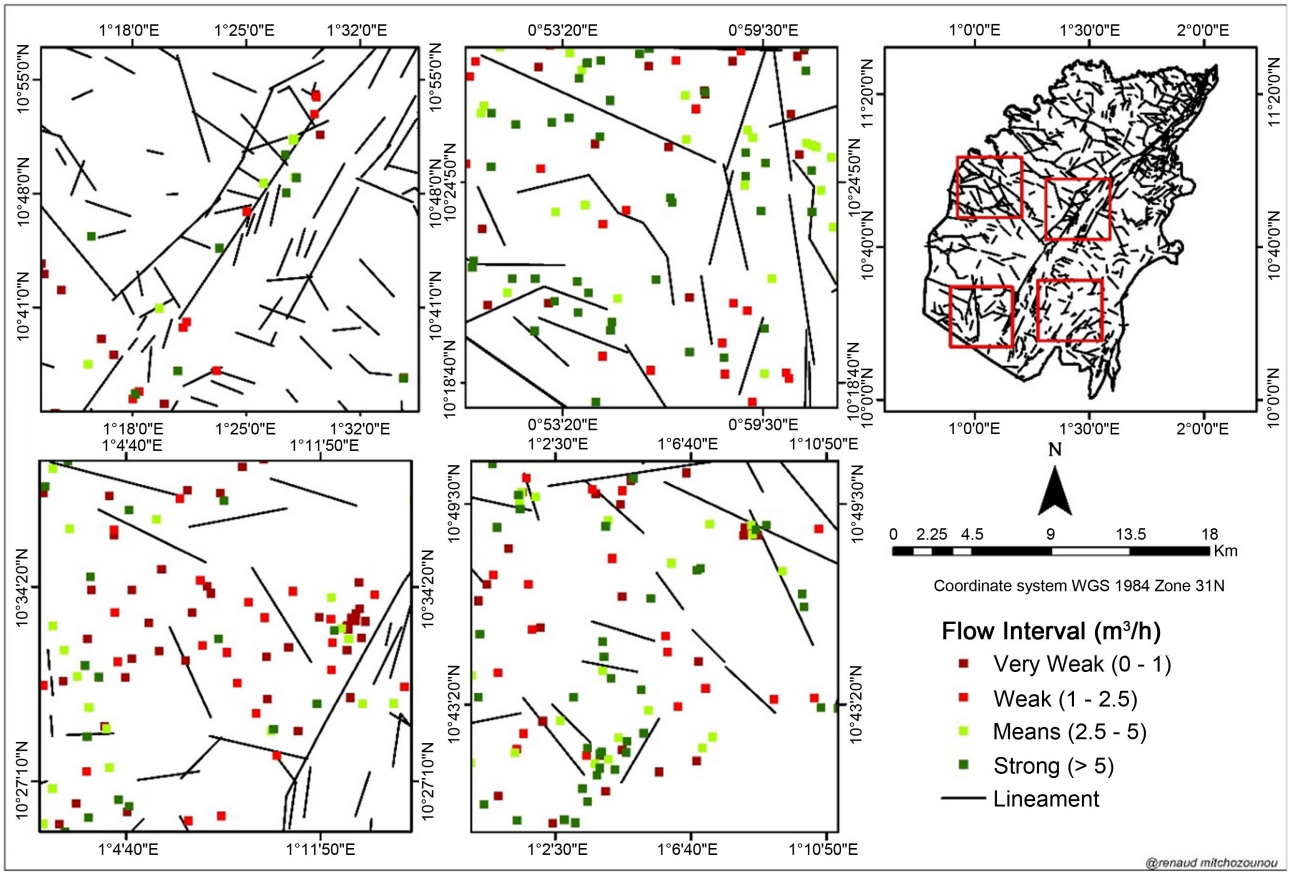

Figure 5. Distribution of operating flows and fracture network in the structural and tectonic units of the Atacora Chain.

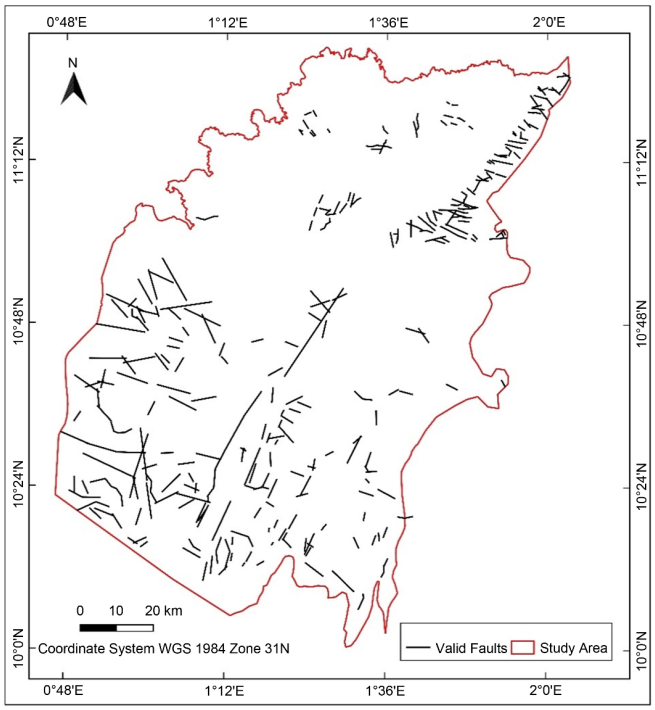

Figure 6. Fractures validated at the scale of the structural and tectonic units of the Atacora Chain.

3. Result

The length of the validated fractures is between 0.33 and 34.10 km. These are classified (Figure 7 and Figure 8) according to the various orientations in the NNE-SSW direction (39 fractures); NE-SW (121 fractures); ENE-OSO (91 fractures); ESE-ONO (146 fractures); SE-NO (15 fractures); and SSE-NNO (5 fractures).

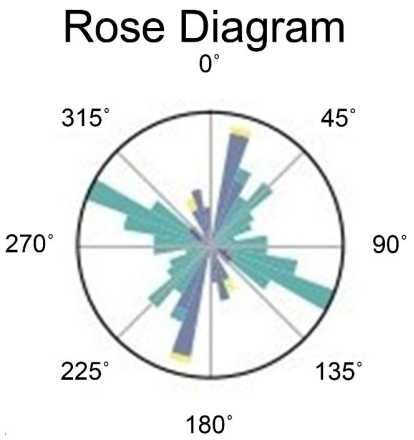

Figure 7. Directionality of identified fractures.

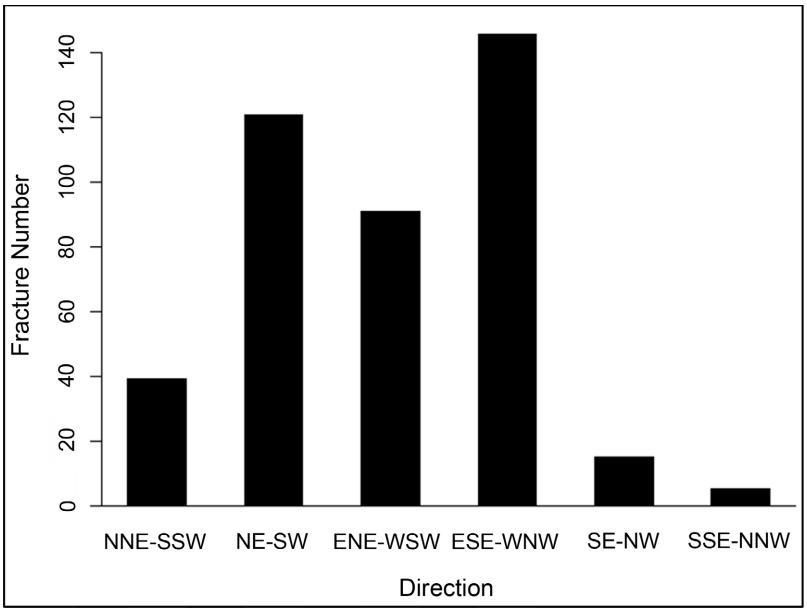

Figure 8. Directional classification of identified fractures.

The graphs in Figure 9 present the distribution of the number of fractures by length class in different directions. The fractures oriented in the NNE-SSW direction are of varied lengths (0.38 - 6.74 km), including 13 with lengths between 0.38 - 1.97 km; 17 whose lengths are between 1.97 - 3.568 km; 7 with lengths between 3.568 - 5.158 km; and 2 whose lengths are between 5.158 km and 6.748 km. The fractures following the NE-SW direction are between 0.35 - 14.41 km. Eighty-one (81) fractures are between 0.32 - 3.853 km, 26 fractures have lengths between 3.85

- 7.37 km, and 11 fractures have lengths between 7.371 - 10.88 km. The major fractures (1.88 - 14.41 km) number 3. Fractures following the ENE-OSW direction (0.5 - 3.9 km and 3.96 - 7.3 km) are 59 and 20 in number, respectively. The major fractures (7.3 - 10.7 km and 10.7 - 14.1 km) number 9 and 3, respectively. The ENE-ONO direction (146 in total) is made up of small fractures between 0.5 - 8.9 km (137 fractures), and 8.9 - 17.3 km (7 fractures). In this direction, the major fractures are not sufficiently represented; the fractures between 17.3 - 25.7 km and 25.7 - 34.10 km are one in number for each length class.

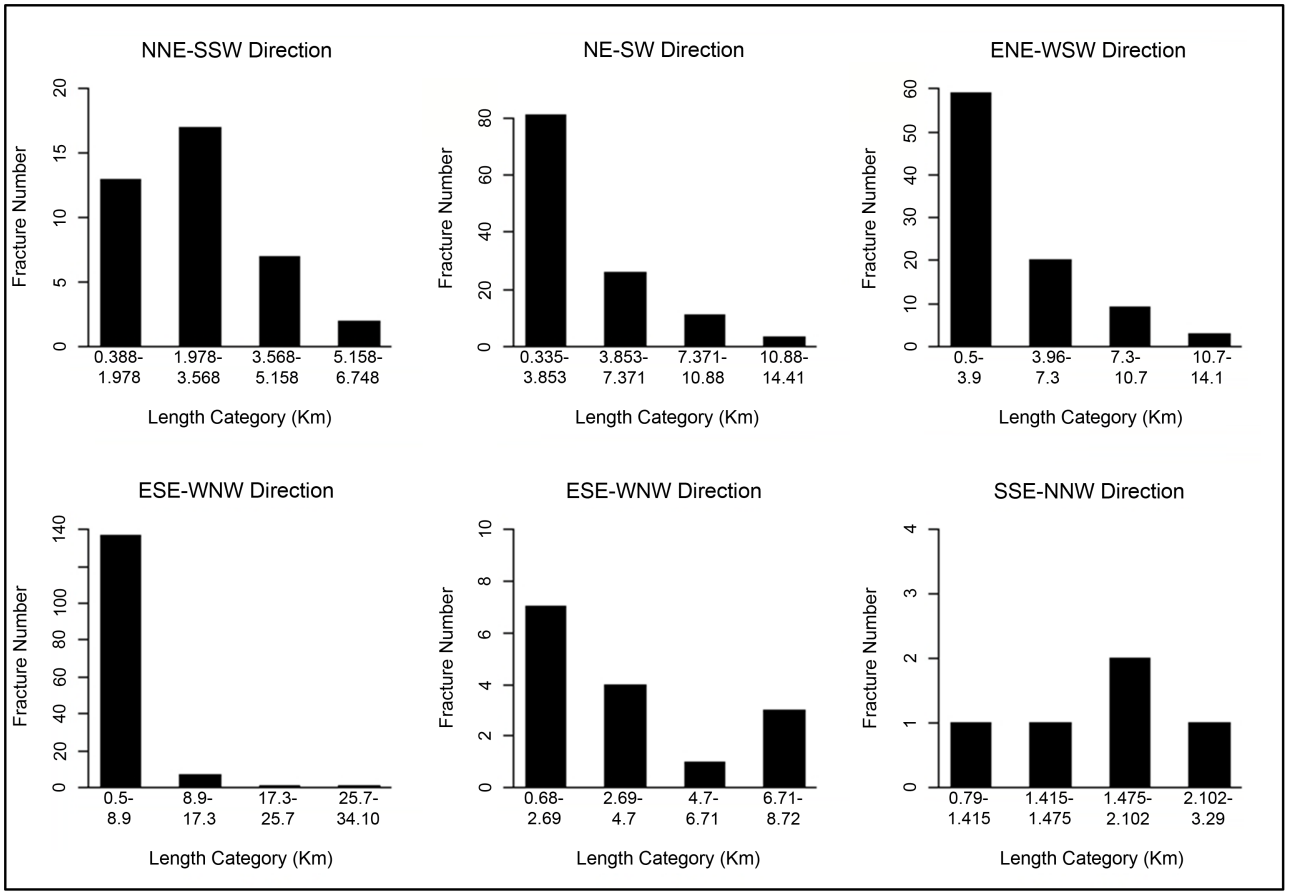

Figure 9. Distribution of the number of fractures by length class in the different directions.

The graphs in **Figure 10** illustrate the classification of the density and number of fractures in the different directions. It appears that the fractures have variable density depending on the orientations. The fractures following the NNE-SSW direction have varying densities, 13 of which have a density between 2.88×10^{-5} - 1.46×10^{-4} km/km^2; 17 with a density between 1.46×10^{-4} - 2.64×10^{-4} km/km^2; 7 with a density between 2.64×10^{-4} - 3.82×10^{-4} km/km^2; and 2 with a density between 3.82×10^{-4} - 5×10^{-4} km/km^2. The fractures following the NE-SW direction have a density between 2.49×10^{-5} - 1.07×10^{-3} km/km^2. Eighty-one (81) fractures have a density between 2.49×10^{-5} - 2.85×10^{-4} km/km^2; 26 fractures have a density between 2.85×10^{-4} - 5.46×10^{-4} km/km^2; and eleven (11) fractures

have a density between 5.46×10^{-4} - 8.07×10^{-4} km/km^2. The densest fractures (8.07×10^{-4} - 1.07×10^{-3} km/km^2) are 03 in number. The fractures following the ENE-OSO direction (3.78×10^{-5} - 2.87×10^{-4} km/km^2 and 2.87×10^{-4} - 5.37×10^{-4} km/km^2) are respectively 59 and 20. The major fractures (5.37×10^{-4} - 7.87×10^{-4} km/km^2 and 7.87×10^{-4} - 1.04×10^{-3} km/km^2) are respectively 9 and 3 in number. The ENE-ONO direction (146 in total) is made up of low-density fractures between 7.87×10^{-5} - 6.53×10^{-4} km/km^2 (137 fractures); 6.53×10^{-4} - 1.2×10^{-3} km/km^2 (7 fractures). In this direction, high-density fractures are not sufficiently represented, fractures between 1.2×10^{-3} - 1.8×10^{-3} km/km^2 and 1.8×10^{-3} - 1.04×10^{-3} km/km^2 are present at the number of one for each fracture density class.

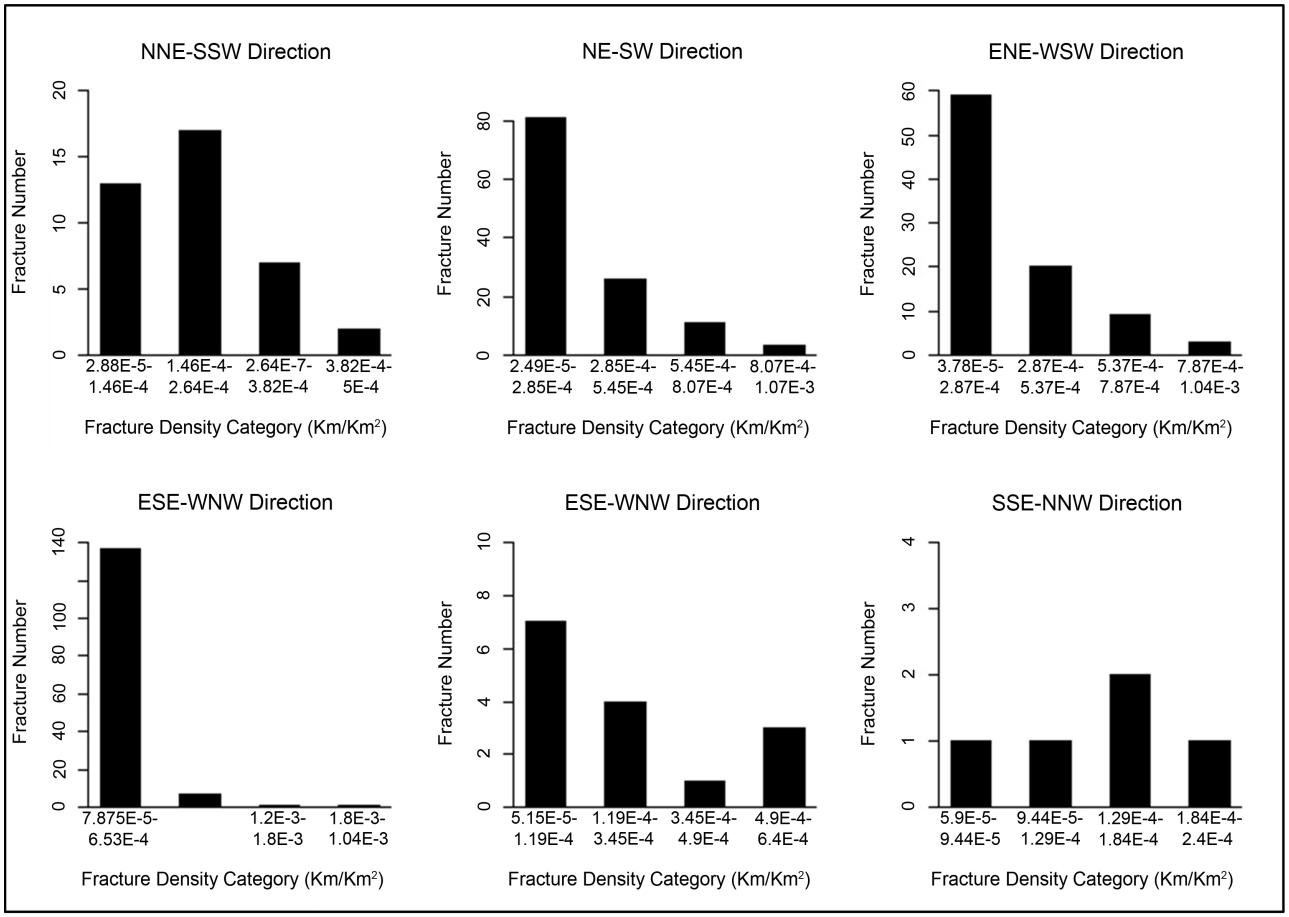

Figure 10. Distribution of the number of fractures by density class according to the different directions.

After analyzing **Figure 9** and **Figure 10**, it is found that in all directions, fractures of long length have a large fracture density, and those of medium and small length have medium and low density.

4. Discussion

The structural and tectonic units contained in the geological formations of the Atacora chain are made up of a large network of fractures. The presence of these fractures could be explained by the tectonic replays observed during the orogeny

of the Pan-African chain of Dahomeyids with the formation of longitudinal, transversal, and oblique fractures [15]. On the scale of the structural and tectonic units of the Atacora chain, the fractures observed are variously oriented, with length (0.33 - 34.10 km) and density (2.45×10^{-5} - 2.50×10^{-3} km/km^2) varied. These results corroborate those obtained by previous work [11] [21] carried out in the crystalline basement of Benin. Unlike the fractures observed in central Benin, which are relatively short, the fractures in the Atacora range are of great length and high density. On the scale of the study sector, the long fractures are located in the South-West part, and those of short length are more localized in the North-East of the study sector. While minor fractures contribute to the overall flow in the aquifers and a certain connectivity, the longest fractures or major fractures have a high linear density which provides high drilling productivity [22] [23]. Drilling is likely to be productive at the interception of two or more fractures, in fracture corridors or in fracturing stars. The density of the fractures ensures high productivity of the drilling to be carried out in the area and plays an important role in the success of the latter. Indeed, it influences the connection of fractures and ensures connectivity between fractures.

5. Conclusion

This study made it possible to dimension elements characterizing the fractures on the scale of the structural units of the Atacora chain through their length, orientation, and density. The fractures observed are variously oriented, with varying length and density. Knowledge of the different characteristics of the fracture network at the scale of the study sector must be used to make more judicious choices in future hydrogeological prospecting campaigns. Knowledge of the directions of fractures can guide hydrogeological prospecting work on the most significant fracture families. Fractures parallel to the direction of the major tectonic stress are better indicated than those perpendicular to this stress. Mapping of tectonic constraints therefore remains to be carried out in order to identify productive drilling points in the structural units of the Atacora chain.

Conflicts of Interest

The authors declare no conflicts of interest regarding the publication of this paper.

References

[1] Kouassi, K. (2012) Evaluation quantitative et qualitative des ressources en eau de la région centre: Cas du département de Didiévi en Côte d'Ivoire. Thèse de Doctorat, Institut National Polytech-nique Félix Houphouet-Boigny de Yamoussoukro.

[2] Jaiswal, R.K., Mukherjee, S., Krishnamurthy, J. and Saxena, R. (2003) Role of Remote Sensing and GIS Techniques for Generation of Groundwater Prospect Zones Towards Rural Development—An Approach. *International Journal of Remote Sensing*, **24**, 993-1008. https://doi.org/10.1080/01431160210144543

[3] Döll, P. and Fiedler, K. (2008) Global-Scale Modeling of Groundwater Recharge. *Hydrology and Earth System Sciences*, **12**, 863-885.

https://doi.org/10.5194/hess-12-863-2008

[4] Affoué, B., Bi Tié, A., Alioune, K., Mangoua, J. and Kouamé, A. (2016) Cartographie du potentiel en eau souterraine du bassin versant de la Lobo (Centre-Ouest, Côte d'Ivoire). Approche par analyse multicritère. *Hydrological Sciences Journal*, **61**, 856-867.

[5] JICA (2018) Rapport de l'étude du concept de base pour le projet d'approvissionnemet en eaau potable dans les régions rurale (phase VI) en République du Bénin.

[6] Darcel, C., Bour, O., Davy, P. and de Dreuzy, J.R. (2003) Connectivity Properties of Two-dimensional Fracture Networks with Stochastic Fractal Correlation. *Water Resources Research*, **39**, 1272-1285. https://doi.org/10.1029/2002wr001628

[7] de Dreuzy, J., Davy, P. and Bour, O. (2001) Hydraulic Properties of Two-Dimensional Random Fracture Networks Following a Power Law Length Distribution: 1. Effective Connectivity. *Water Resources Research*, **37**, 2065-2078. https://doi.org/10.1029/2001wr900011

[8] Bour, O. and Davy, P. (1997) Connectivity of Random Fault Networks Following a Power Law Fault Length Distribution. *Water Resources Research*, **33**, 1567-1583. https://doi.org/10.1029/96wr00433

[9] Davy, P., Sornette, A. and Sornette, D. (1990) Some Consequences of a Proposed Fractal Nature of Continental Faulting. *Nature*, **348**, 56-58. https://doi.org/10.1038/348056a0

[10] Nesny, A.Y., Nicaise, Y., Bertrand, A.H., Marc, Y.T. and George, A. (2019) Apport de la télédétection et de la géophysique dans la cartographie des fractures hydrauliquement actives en zone de socle au Centre-Ouest du Benin. *European Scientific Journal ESJ*, **15**, 426-447. https://doi.org/10.19044/esj.2019.v15n27p426

[11] Oussou, M.A, F.E., Oloukoi, J., Yalo, N. and Boukari, M. (2019) Analyse Spatiale du Potentiel en eau Souterraine dans le Bassin du Zou au Sud du Benin (Afrique de L'ouest). *European Scientific Journal ESJ*, **15**, 402-425. https://doi.org/10.19044/esj.2019.v15n27p402

[12] Ake, G.E., Kouame, K.J., Koffi, A.B. and Jourda, J.P. (2018) Cartographie des zones potentielles de recharge de la nappe de Bonoua (sud-est de la Côte d'Ivoire). *Revue des sciences de l'eau*, **31**, 129-144. https://doi.org/10.7202/1051696ar

[13] Koita, M., Jourde, H., Ruelland, D., Koffi, K., Pistre, S. and Savane, I. (2010) Cartographie des accidents régionaux et identification de leur rôle dans l'hydrodynamique souterraine en zone de socle. Cas de la région de Dimbokro-Bongouanou (Côte d'Ivoire). *Hydrological Sciences Journal*, **55**, 805-820. https://doi.org/10.1080/02626667.2010.489749

[14] Avy, S., Koffi, G., Kouassi, E. and Yenipoho, G. (2021) Extraction par la Teledetection du Reseau de Fractures. *American Journal of Innovative Research and Applied Sciences*, **12**, 1-12.

[15] Affaton, P. (1975) Etude géologique et structurale du Nord-Ouest Dahomey, du Nord-Togo et du Sud-Est de la Haute-Volta. Ph.D. Thesis, Université Aix-Marseille-3 Paul Cézanne.

[16] Pascal, A. (1990) Le bassin des volta (afrique de l'ouest): Une marge passive, d'âge protérozoïque supérieur, tectonisée au panafricain (600 f 50 Ma). Institut français de re-cherche scientifique pour le développement en coopéfuttion.

[17] Biémi, J. (1992) Contribution à l'étude géologique, hydrogéologique et par télédétection des bassins versants sub-sahéliens du socle précambrien d'Afrique de l'Ouest: Hydrostructurale, hydrodynamiquehydrochimie et isotopie des aquifères discontinus

de sillons et aires. 493 p.

[18] Kanohin, O., Saley, B., Aké, G. and Savané, I. (2012) Apport de la télédétection et des SIG dans l'identification des ressources en eau souterraine dans la région de Daoukro (Centre-Est de la Côte d'Ivoire). *International Journal of Innovation and Applied Studies*, **1**, 35-53.

[19] Ouedraogo, M. (2016) Caractérisation des aquifères de socle pour l'amélioration de la productivité des forages d'hydraulique villageoise dans le bassin versant du Bandama blanc amont (Nord de la Côte d'Ivoire). Thèse de doctorat, Université Paris-Saclay.

[20] Jourda, J., Saley, M.B., Djagoua, E.V., Kouame, K.J., Biemi, J. and Razack, M. (2006) Utilisation des données ETM+ de Landsat et d'un SIG pour l'évaluation du potentiel en eau souterraine dans le milieu fissuré précambrien de la région de de Korhogo (nord de la Côte d'Ivoire): Approche par analyse multicritère et test de validation. *Revue de Télédétection*, **5**, 339-357.

[21] Akame, J., Ondoa, J., Olinga, J.B., Essono, J. and Kemeng, P. (2013) Utilisation des modèles numériques de terrain (MNT) SRTM pour la cartographie des linéaments structuraux: Application à l'Archéen de Mezesse à l'est de Sangmélima (Sud-Cameroun). Geo-Eco-Trop.

[22] Engalec, M. (1982) Rôle photo-interprètation dans la détermination des facteurs influençant la productivité des fractures du socle cristallin.

[23] Ronteix, S. (1986) La fracturation des roches dures et la prospection hy-drogéologique. Bureau de recherche géologique et minière.